ISNN:2181-1296

SHAROF RASHIDOV NOMIDAGI
SAMARQAND DAVLAT UNIVERSITETI

САМАРКАНДСКИЙ ГОСУДАРСТВЕННЫЙ
УНИВЕРСИТЕТ ИМЕНИ ШАРОФА РАШИДОВА

SAMARKAND STATE UNIVERSITY NAMED
AFTER SHAROF RASHIDOV

ILMIY AXBOROTNOMA

НАУЧНЫЙ ВЕСТНИК
SCIENTIFIC JOURNAL

ANIQ VA TABIIY FANLAR SERIYASI

Matematika, Mexanika, Informatika
Fizika, Kimyo, Biologiya, Geografiya

№ 1/2 (155)
2026

ISSN 2181-1296

ILMIY AXBOROTNOMA

НАУЧНЫЙ ВЕСТНИК SCIENTIFIC JOURNAL

2026-yil, 1-son (155/2) ANIQ VA TABIIY FANLAR SERIYASI

Matematika, Mexanika, Informatika, Fizika, Kimyo, Biologiya, Geografiya

Samarqand viloyat matbuot boshqarmasida ro‘yxatdan o‘tish tartibi 09-25.
Jurnal 1999-yildan chop qilina boshlagan va OAK ro‘yxatiga kiritilgan.

BOSH MUHARRIR **R. I. XALMURADOV, t.f.d., professor**
BOSH MUHARRIR O‘RINBOSARLARI: **H.A. XUSHVAQTOV, f-m.f.d., dotsent**

TAHRIRIYAT KENGASHI:

Sh.A.Alimov	- O‘zFA akademigi	**M.X.Ashurov**	- O‘zFA akademigi
S.N.Lakayev	- O‘zFA akademigi (SamDU)	**B.J.Axmedov**	- O‘zFA akademigi
M.M.Kamilov	- O‘zFA akademigi	**Q.G‘.G‘ulomov**	- O‘zFA akademigi
A.G.Yagola	- Moskva davlat universiteti professori (Rossiya)	**A.A.Zaxidov**	-Texas Nanotexnologiya instituti professori (AQSh)
Alberto Del Bimbo	-Florensiya universiteti professori (Italiya)	**N.B. Ferapontov**	- Moskva davlat universiteti professori (Rossiya)
Sh.Tugizov	-Kaliforniya universiteti professori (AQSh)	**V.L.Popov**	-Berlin texnika universiteti professori (Germaniya)
A.S.Soleev	- f.-m.f.d., professor (SamDU)	**N.F.Bunkin**	- Moskva davlat texnika universiteti professori (Rossiya)
I.A.Ikromov	- f.-m.f.d., professor (SamDU)	**Haji Akber Aisa**	-Xinjiang tibbiyot universiteti professori (Xitoy)
B.X.Xo‘jayarov	- f.-m.f.d., professor (SamDU)	**E. A. Abduraxmonov**	- k.f.d., professor (SamDU)
L.Sabirov	-f.-m.f.d., professor (SamDU)	**N. K. Muxamadiyev**	- k.f.d., professor (SamDU)
A.Jumaboyev	-f.-m.f.d., professor (SamDU)	**L. A. Bulavin**	- Kiev milliy universiteti
X.Bozorov	-k.f.d., professor (SamDU)	**X. Q. Xaydarov**	- b.f.d., professor (SamDU)
O.Q.Quvondiqov	-f.-m.f.d. professor (SamDU)	**Z. I. Izzatullayev**	- b.f.d., professor (SamDU)
A.Z.Xasanov	-f.-m.f.d. professor (SamDU)	**A.B.Hasanov**	-tex.f.d., professor (SamDU)
Muhammad Suzuri bin Hitam	- Terengganu universiteti professori (Malayziya)	**Sh. T. Xoliqulov**	- q.-x.f.d., professor (SamDU)
K.D.Kuliyev	- f.-m.f .n. professor (SamDU)	**S. B. Abbosov**	- g.f.d., professor (SamDU)
A.M.Xolxo‘jayev	-f.-m.f.d., professor (SamDU)	**M.E. Mo‘minov**	-f.-m.f.d., professor (SamDU)
J.Abdullayev	-f.-m.f.d., professor (SamDU)	**I.I.Jumanov**	-tex.f.d., professor (SamDU)
A.R.Axatov	-tex.f.d., professor (SamDU)	**N.S.Mamatov**	-tex.f.d., professor (TIQXMMI)
D.B.Xursanov	- g.f.f.d., dotsent (SamDU)	**A.Sh.Yarmuxamedov**	-f-m.f.n., dotsent (SamDU)
F.Nazarov	-tex.f.d., dotsent (SamDU)	**X.S.Xaydarov**	-f-m.f.n., dotsent (SamDU)

Obuna indeksi – yakka tartibdagi obunachilar uchun **- 5583,**
tashkilot, korxonalar uchun **- 5584**

M U N D A R I J A
C O N T E N T S

№	Maqola nomi	Article title	Bet/ page
1.	Yuqori chastotali II-turdagi radio portlash spektral kuzatuvlaridan foydalanib magnit maydon kuchini baholash **Pulatov D., Mirtoshev Z.**	Estimation Of The Coronal Magnetic Field Strength Using High-Frequency Type Ii Radio Burst Observations **Pulatov D., Mirtoshev Z.**	**5-11**
2.	Rayxon (OCIMUM) o‘simligi efir moyi kimyoviy tarkibiga iqlim omillarining ta’sirini GX–MS usulida tadqiq etish **Siddikova Y., Saifullaeva Sh., Mukhamadiyev A., N.Fazlieva, Nayimova B., Muhamadiyev N.**	Study of the influence of climate factors on the chemical composition of basil (ocimum) essential oil using the GH–MS method **Siddikova Y., Saifullaeva Sh., Mukhamadiev A., N.Fazlieva, Nayimova B., Muhamadiev N.**	**12-20**
3.	Bentonitni montmorillonit bilan boyitishning samarali usullari va termal ishlov berishning kation almashinuvi quvvatiga ta'siri **Mamadoliev I., Abdikamalova A., Ruzieva S.**	Effective methods for bentonite enrichment with montmorillonite and the impact of thermal treatment on cation exchange capacity **Mamadoliev I., Abdikamalova A., Ruzieva S.**	**21-28**
4.	$KPbBr_3$ asosidagi peroled tuzilmalarida zaryad tashish mexanizmlari va energetik sathlarning moslashuvi **Rahmonova M., Muxamadiyev N.**	Charge transport mechanisms and energy level alignment in $KPbBr_3$ -based peroled structures **Rahmonova M., Mukhamadiev N.**	**29-36**
5.	*N*-(4-(((7-Nitroxinazolin-4-il) amino) metil)fenil) siklogeksankarboksamid sintezi **Gaybullaev Sh., Takhirov Y., Chao Niu, Bozorov Kh.**	Synthesis of N-(4-(((7-nitroquinazolin-4-YL) amino) methyl) phenyl) cyclohexanecarboxamide **Gaybullaev Sh., Takhirov Y., Chao Niu, Bozorov Kh.**	**37-41**
6.	3-brom-pirido[2,3-*d*]pirimidinonlarning sintezi **Khushnazarov Z., Turgunov D., Bozorov Kh.**	synthesis of 3-bromo-pyrido[2,3-d]pyrimidinones **Khushnazarov Z., Turgunov D., Bozorov Kh.**	**42-46**
7.	Zarrachalar tezlatkichlarida materiallarning aktivatsiyasi va radiatsion xavflar **Temirov J., Khasanov Sh., Safarov A., Karimberganova Q.**	Material activation and radiological hazards in particle accelerators **Temirov J., Khasanov Sh., Safarov A., Karimberganova Q.**	**47-57**
8.	Geoinformatsion dasturlar yordamida demografik atlaslar yaratishning afzalliklariga nazar **Tukhtamishev Sh., Khudoyarova Sh., Shirinboyev D.**	Advantages of creating demographic atlases using geoinformation software **Tukhtamishev Sh., Khudoyarova Sh., Shirinboev D.**	**58-62**
9.	Siklopropilatsetilen asosida atsetilen spirtlari sintezi, ularning nazariy energetik xarakteristikalari va nadfoksidaza oqsili (7U8G) bilan molekulyar birikish tahlili **Ziyadullaev M.E., Nurmanov S.E., Buriev F.Kh., Abdukhalikov F.J.**	Synthesis of acetylenic alcohols based on cyclopropylacetylene, their theoretical energetic characterization, and molecular docking analysis with nadph oxidase (7U8G) protein **Ziyadullaev M.E., Nurmanov S.E., Buriev F.Kh., Abdukhalikov F.J.**	**63-71**
10.	Tetratsiklik tieno[3,2-*d*]pirimidinonlarning siklooksigenaza-2 ingibitorlari sifatida *in silico* tadqiqi **Nasrullaev A., Buronov A., Gaybullaev Sh., Bozorov Kh.**	In silico evaluation of tetracyclic thieno[3,2-d]pyrimidinones as potential cyclooxygenase-2 inhibitors **Nasrullaev A., Buronov A., Gaybullaev Sh., Bozorov Kh.**	**72-76**
11.	H3PO4, KOH va ZnCl2 yordamida olingan faollashtirilgan ko‘mirning morfologik va strukturaviy xususiyatlarining qiyosiy tahlili **Ergasheva D., Mukhamadiyev A., Mukhamadiyev N., Uzokov J.**	Comparative analysis of the morphological and structural properties of activated carbon prepared using H_3PO_4, KOH, and $ZnCl_2$ **Ergasheva D., Mukhamadiev A., Mukhamadiev N., Uzokov J.**	**77-81**
12.	CO_2 NI quyosh nuri ta’sirida samarali konversiyalashni ta’minlovchi g-C_3N_4/$CoNi_2S_4$ geterotuzilmali nanomateriallar sintezi va fizik-kimyoviy xossalari **Samiev A., Nizamov U.N., Mirzaev Sh., Ruzimuradov O., Nasimov A.**	Synthesis and physicochemical properties of γ-C3N4/CoNi2S4 heterostructured anomaterials providing efficient conversion of CO2 under the influence of sunlight **Samiev A., Nizamov U.N., Mirzaev Sh., Ruzimuradov O., Nasimov A.**	**82-87**

№	Maqola nomi	Article title	Bet/ page
13.	Atrof muhitdagi ammiak mikrokensentratsiyasini monigitori uchun gibrid perovskit $MA_xFA_{1-x}PbI_3$ fluoressent sensori tayyorlash **Eshmuradova G.B., Tashpulatov Kh.Sh., Khursandov J.M., Normuradov O.U., Norboyev Q.M., Toshpulatov D.T.**	Preparation of hybride perovskite $MA_xFA_{1-x}PbI_3$-fluorescent sensor for the monitoring of ammonia microconcentration in environment **Eshmuradova G.B., Tashpulatov Kh.Sh., Khursandov J.M., Normuradov O.U., Norboev Q.M., Toshpulatov D.T.**	**88-92**
14.	Al^{3+} bilan modifikatsiyalangan shpinel tuzilishga ega $Li_{1.33}Al_XMn_{1.67-X}O_4$ ($0 \leq x < 0.7$) tarkibli adsorbentlarning zol-gel sintezi va fizik-kimyoviy xossalari **Begimkulova Sh.A., Nematova Sh.Sh., Baxriev I.S., Mirzaev Sh.E., Ruzimuradov O.N., Nasimov A.M.**	Sol-gel synthesis and physicochemical properties of adsorbents consisting of Al^{3+} modified spinel structure $LI_{1.33}Al_XMn_{1.67-X}O_4$ ($0 \leq X < 0.7$) **Begimkulova Sh.A., Nematova Sh.Sh., Baxriev I.S., Mirzaev Sh.E., Ruzimuradov O.N., Nasimov A.M.**	**93-99**
15.	CdCr2Se4 va CuCr4Se4 magnitli yarimo‘tkazgichda magnit-optik effektlar **Dosmurodov G.**, **Kurbaniyazov A.**, **Boboqambarova G.**	Magneto-optical effects in the magnetic semiconductor CdCr2Se4 AND CuCr4Se4 **Dosmurodov G.**, **Kurbaniyazov A.**, **Bobokambarova G.**	**100-104**
16.	Sophora lehmanni va Cicer mogoltavikum o‘simliklari yer ustki qismilarining flavonoidlari **Gafurov A.Zh, Botirov E. Kh.**	Flavonoids of aerial parts of sophora lehmannii and cicer mogoltavicum **Gafurov A.Zh, Botirov E. Kh.**	**105-109**
17.	Buxoro viloyatining balneologik resurslari va ularning aholi salomatligini yaxshilashdagi ahamiyati **Zaynutdinova D.K., Nematova Kh. Kh.**	Balneological resources of the bukhara region and their significance in improving public health **Zaynutdinova D.K., Nematova Kh. Kh.**	**110-116**
18.	Tabiiy cho‘kuvchan gruntlarni polimer-kompozitsion eritmalar bilan inyeksion mustahkamlash texnologiyasini matematik rejalashtirish **Bakhriyev N.F., Kholiqulov O.O., Nurmatova R.K.**	Mathematical planning of injection strengthening technology of natural collapsible soils using polymer-composite solutions **Bakhriyev N.F., Kholikulov O.O., Nurmatova R.K.**	**117-125**
19.	Adgezion kontaktlarda ishqalanish koeffitsiyentiga geometrik parametrlar hamda tashqi yuk ta’sirining tahlili **Bekmamatova G., Xoliqulov O., Tojinorov M.**	Analysis of geometric parameters and external load on the friction coefficient in adhesive contacts **Bekmamatova G., Xolikulov O., Tojinorov M.**	**126-131**
20.	Markaziy Osiyo iqlim sharoitida sorbsion sovutgichlardan biogaz komplekslari bilan simbiozda foydalanish istiqbollari **Abdusamiyev F., Bahriev S., Sattarov S.**	Prospects for using sorption refrigerators in symbiosis with biogas complexes in the climatic conditions of Central Asia **Abdusamiev F., Bahriev S., Sattarov S.**	**132-136**
21.	Maple tizimida algebraik ko’pxilliklarni ratsional parametrlashining nazariy asoslari va kompyuterda amalga oshirilishi **Usmonova N.**	Theoretical foundations and computer implementation of rational parameterization of algebraic manifolds in the maple system **Usmonova N.**	**137-142**
22.	$Fe_5Ga_6Gd_2YZr$ ko‘p komponentli kristallining element tarkibi va tebranish xossalarini rentgen-fluoresans (XRF) va raman spektroskopiyasi yordamida tadqiq etish **Nasirova N., Fayziyev Sh., Saidov Q., Qaxorova Sh., Sharipov M., Djuraev D.**	Investigation of the elemental composition and vibrational properties of the multicomponent crystal Fe5Ga6Gd2YZr using X-RAY fluorescence (XRF) and raman spectroscopy **Nasirova N., Fayziyev Sh., Saidov Q., Qaxorova Sh., Sharipov M., Djuraev D.**	**143-152**
23.	Xofp tipidagi tenglamalar sistemasi uchun Koshi masalasi **Erkinova D. A.**, **Imomnazarov Kh. Kh.**	Cauchy problem for a Hopf-type system **Erkinova D. A.**, **Imomnazarov Kh. Kh.**	**153-157**
24.	Ar va HCl izotopologlari o‘rtasida hosil bo‘lgan komplekslarning kvant-kimyoviy tahlili: AIM, RDG va NCI usullari yordamida solvatatsiya effektlarini o‘rganish **Khujamov U.**	Quantum-chemical analysis of complexes formed between Ar and HCL isotopologues: studying solvation effects using AIM, RDG, and NCI methods **Khujamov U.**	**158-167**

UDC: 537.632.4 https://doi.org/10.59251/2181-3973.2025.v1.138.1.3835

INVESTIGATION OF THE ELEMENTAL COMPOSITION AND VIBRATIONAL PROPERTIES OF THE MULTICOMPONENT CRYSTAL Fe5Ga6Gd2YZr USING X-RAY FLUORESCENCE (XRF) AND RAMAN SPECTROSCOPY

N.Nasirova, Sh.Fayziyev, Q.Saidov, Sh.Qaxorova, M.Sharipov, D.Djuraev
Bukhara state university, Bukhara, Uzbekistan.

N.Nasirova Bukhara state university, Bukhara, Uzbekistan.

Received: 30.01.2026
Revised: 22.02.2026
Accepted: 26.02.2026
Published: 30.03.2026

Publisher: Samarkand State University named after Sharof Rashidov.

Abstract. In this work, the elemental composition and vibrational properties of the multicomponent crystal $Fe_5Ga_6Gd_2YZr$ were investigated using X-ray fluorescence analysis (XRF) and Raman spectroscopy. The XRF results enabled the identification of the main elements present in the sample and their relative proportions. Raman spectroscopy was used to analyse the interatomic vibrations in the crystal lattice, identifying phonon modes associated with heavy atoms in the low-frequency region and vibrations corresponding to the Fe–Ga and Fe–Zr bonds in the medium-frequency range. The results obtained indicate that the $Fe_5Ga_6Gd_2YZr$ crystal possesses complex vibrational dynamics, allowing it to be evaluated as a multicomponent material with functional properties.

Keywords: $Fe_5Ga_6Gd_2YZr$; multicomponent crystal; Raman spectroscopy; X-ray fluorescence analysis (XRF); elemental composition; phonon modes; vibrational properties; interatomic interactions.

$Fe_5Ga_6Gd_2YZr$ ko‘p komponentli kristallining element tarkibi va tebranish xossalarini rentgen-fluoresans (xrf) va raman spektroskopiyasi yordamida tadqiq etish

Annotatsiya. Ushbu ishda $Fe_5Ga_6Gd_2YZr$ ko‘p komponentli kristallining element tarkibi va tebranish xossalari rentgen-fluoresans tahlili (XRF) hamda Raman spektroskopiyasi yordamida tadqiq etildi. XRF natijalari namunadagi asosiy elementlarning mavjudligini va ularning nisbiy ulushlarini aniqlash imkonini berdi. Raman spektroskopiyasi yordamida kristall panjaradagi atomlararo tebranishlar tahlil qilinib, past chastota sohasida og‘ir atomlar bilan bog‘liq fonon modalar, o‘rta chastota diapazonida Fe–Ga va Fe–Zr bog‘lanishlariga mos tebranishlar aniqlandi. Olingan natijalar $Fe_5Ga_6Gd_2YZr$ kristallining murakkab tebranish dinamikasiga ega ekanligini ko‘rsatadi va uni funksional xossalarga ega ko‘p komponentli material sifatida baholash imkonini beradi.

Kalit so‘zlar: $Fe_5Ga_6Gd_2YZr$; ko‘p komponentli kristall; Raman spektroskopiyasi; rentgen-fluoresans tahlili (XRF); element tarkibi; fonon modalar; tebranish xossalari; atomlararo o‘zaro ta’sirlar.

Исследование элементного состава и колебательных свойств многокомпонентного кристалла $Fe_5Ga_6Gd_2YZr$ методами рентгенофлуоресцентного анализа и рамановской спектроскопии

Аннотация. В работе исследованы элементный состав и колебательные свойства многокомпонентного кристалла $Fe_5Ga_6Gd_2YZr$ методами рентгенофлуоресцентного

анализа (XRF) и рамановской спектроскопии. Результаты XRF позволили определить наличие основных элементов в образце и их относительное содержание. С помощью рамановской спектроскопии проанализированы атомные колебания в кристалле: в низкочастотной области выявлены фононные моды, связанные с тяжёлыми атомами, а в среднем диапазоне — колебания, соответствующие связям Fe–Ga и Fe–Zr. Полученные данные свидетельствуют о сложной колебательной динамике кристалла $Fe_5Ga_6Gd_2YZr$ и подтверждают перспективность данного материала для дальнейших исследований его функциональных свойств.

Ключевые слова: $Fe_5Ga_6Gd_2YZr$, многокомпонентный кристалл, рамановская спектроскопия, рентгенофлуоресцентный анализ (XRF), элементный состав, фононные моды, колебательные свойства, межатомные взаимодействия.

Introduction. In recent years, the study of optical phenomena and their effects on crystal structures has remained one of the most pressing areas of modern physics. Crystals, particularly ferromagnetic and ferroelectric materials, are distinguished by their domain structure. Domains are small regions within the crystal that possess uniformly aligned magnetic or electric moments [1]. The variation of such domains can occur under the influence of external factors, including light radiation[2].

The effect of light on the crystal structure is usually manifested through photo-induction processes. The energy carried by the photon interacts with the interparticle bond forces in the crystal lattice, leading to the displacement of domain boundaries or the formation of new domains. [3]. As a result, the material's magnetic, electrical and optical properties change. This phenomenon is observed through processes such as the photoferroelectric effect, the photomagnetic effect or photochromism[4].

Numerous studies have shown that the reorganisation of the domain structure under the influence of light depends on the crystal's energy state, temperature, and the wavelength and intensity of the light [5]. For example, in some ferroelectric crystals, the movement of domain walls is accelerated by ultraviolet radiation, which alters their dielectric response[6].

The relevance of this topic lies in the fact that studying the change in domain structure under the influence of light provides a theoretical basis for the creation of new photoactive materials, optical memory elements, and energy-efficient sensor systems [7]. Therefore, the experimental and theoretical analysis of the effect of light on the domain structure of crystals is currently considered one of the most promising directions in physics.

The unique crystallographic and electronic structures of complex intermetallic compounds such as $Fe_5Ga_6Gd_2YZr$ make them promising materials for advanced technological applications, which necessitates a comprehensive and in-depth study of their fundamental physical properties. Research on high-entropy and compositionally complex alloys has given rise to a new class of metallic materials with superior mechanical properties, establishing them as systems of significant importance in the design of modern alloys. [8]. Typically composed of five or more principal elements in atomic ratios close to unity, these alloys exhibit high strength, high hardness, excellent resistance to corrosion and fracture, and stability at high temperatures, demonstrating significant advantages over conventional alloys [9]. Recent studies have extensively highlighted the importance of X-ray fluorescence spectroscopy (XRF) in analysing the elemental composition of multiphase systems such as $Fe_5Ga_6Gd_2YZr$. This method offers high accuracy in determining the qualitative and quantitative composition of elements and is distinguished by its non-destructive analysis capability [10]. As noted in the literature, the XRF technique is based on the principle of detecting element-specific fluorescent radiation produced by high-energy X-rays, which enables the reliable identification of each element [11]. It has been noted that the quantitative data obtained via XRF play a crucial role in elucidating the formation and stability of phases in high-entropy and complex intermetallic materials [12].

Furthermore, the authors have shown that these compositional analysis results play a crucial role in establishing correlations with macroscopic properties and in developing combinatorial approaches aimed at the search for new, high-performance alloys [13]. Raman spectroscopy is widely used as an indispensable analytical method for investigating vibrational properties, crystal structure, and phase transitions in complex, multicomponent materials [14]. In the literature, this method has been used to study phonon modes, has been noted to provide high-resolution information on lattice distortions and chemical bonds, and this information is crucial for elucidating the complex interrelationship between composition, structure, and functional properties. In particular, Raman spectroscopy provides important insights into the local atomic positions, the vibrational modes associated with the various elemental components, and their interactions within the $Fe_5Ga_6Gd_2YZr$ crystal lattice [15].

Fundamental Principles and Analytical Methods of XRF and Raman Spectroscopy. X-ray fluorescence (XRF) analysis is a reliable analytical method used to identify and quantify the elements in a material. This method is based on detecting the characteristic secondary radiation produced when the material is excited by X-rays.

When the sample is irradiated with high-energy primary X-rays, electrons from the inner shell of an atom are ejected. The resulting vacant energy level is filled by electrons from a higher-energy level, and in this process characteristic X-rays are generated. The energy of these quanta is characteristic of the element, allowing each element to be identified. The device's energy-sensitive detector determines the energy of each photon individually and records it as a complete spectrum.

The fundamental parameters method was used to perform quantitative analysis based on the resulting spectrum. This method is based on fundamental physical laws and atomic constants, taking into account photoionisation cross-sections, fluorescence emission probability, mass absorption coefficients, geometric factors, and detector efficiency, and therefore operates with minimal dependence on calibration standards.

The main advantage of the fundamental parameter method is that it provides reliable results even for multi-component and complex matrix samples. The fluorescence intensity recorded for sample *"i"* is determined by the following expression:

$$I_i = K \cdot C_i \cdot \sigma_i(E_0) \cdot \omega_i \cdot G \cdot e^{-\mu_m d} \qquad (1)$$

where: C_i - mass fraction of the element, σ_i - cross section for photoionisation, ω_i - probability of fluorescence emission, G - factors arising from the sample's geometric dimensions; μ_m - the matrix absorption coefficient; d – the sample thickness; K – a proportionality constant depending on the experimental setup.

The fundamental parameter algorithm determines the concentrations of all elements by iteratively solving equation (1). In XRF analysis, matrix effects (absorption and secondary excitation) play an important role. In the fundamental parameter method, the absorption of one element's radiation by another and the attenuation of light-element signals by heavy elements are fully mathematically modelled. This is particularly important for complex alloys and phase-transition materials.

Raman spectroscopy was also employed for structural analysis. Raman spectroscopy is one of the most effective optical analysis techniques, providing information about the vibrational, rotational, and lattice (phonon) states (spectra) of materials. This method is based on the phenomenon of inelastic scattering, which occurs as a result of the interaction between light and matter. When a monochromatic laser beam is directed at the sample, a small fraction of the scattered photons returns with an energy exchange, and this energy difference is recorded as a frequency shift.

Frequency shift is determined by the following expression:

$$\Delta\nu = \nu_0 - \nu_S \qquad (2)$$

ν_0 - frequency of the incident laser beam, ν_S - frequency of the scattered light.

Emission-accompanied scattering corresponds to Stokes components, while energy-uptake-accompanied scattering corresponds to anti-Stokes components. In practical analyses, Stokes lines are primarily studied due to their high intensity.

Active vibrations in the Raman spectrum are associated with changes in the material's polarisation tensor. If the polarisation of the molecule or of the crystal unit cell changes during the vibration process, that vibration is observed in the Raman spectrum. For this reason, Raman spectroscopy is particularly effective in detecting structures that lack central symmetry or have broken local symmetry.

In crystals, Raman-active phonon modes are determined on the basis of group theory. For each crystal symmetry group, there is a specific number and type of Raman-allowed spectral modes, which manifest as distinct peaks in the observed spectrum.

Thus, Raman spectroscopy is a reliable and informative method for determining the vibrational states of the crystal lattice, the phonon modes, and the local and global symmetry properties. Changes in the Raman spectrum allow for a detailed analysis of spatial transitions, structural distortions, and interatomic interaction mechanisms.

Materials and methods. The fundamental parameters of the $Fe_5Ga_6Gd_2YZr$ crystal were measured using a Rigaku NEX DE instrument. The experiment was carried out under standard conditions (ambient air) without rotating the sample.

X-ray fluorescence (XRF) spectroscopy measurements were performed under conditions automatically set by the instrument, including voltage, current, filter type, and measurement time. The obtained spectra were used for further quantitative analysis based on the fundamental parameters method.

Table 1

ode	Filter	Voltage (kV)	Current (μA)	Measurement time (s)	Time percentage (%)
ow-Z	Open	6.5	296	100	36.9
id-Z	C	35.0	107	100	37.2

Raman spectroscopy was employed to investigate the vibrational properties of the crystal structure in the spectral range of 400–4000 cm^{-1}.

Results and discussion. The quantitative analysis of the XRF spectra revealed that the main components of the $Fe_5Ga_6Gd_2YZr$ compound are Fe, Ga, Zr, Gd, and Y. The elemental composition in molar percentages is presented in Table 2.

Composition of the sample by elements (mol %)

Table 2

	Element	Quantity (mol %)	Spectral line	Intensity (cps/μA)
	Ga	39.8	Ga–Kα	186.54
	Fe	32.4	Fe–Kα	64.27
	l	11.4	Gd–Lα	21.48
	Y	9.41	Y–Kα	136.97
	Zr	7.05	Zr–Kα	110.37

The spectrum exhibits characteristic peaks corresponding to Gd-L lines (6–8 keV), Fe-Kα (6.4 keV), Ga-Kα and Ga-Kβ (9–10 keV), as well as Y-Kα and Zr-Kα peaks in the 14–16 keV range. The distinctness of these peaks confirms the reliable identification of the constituent elements.

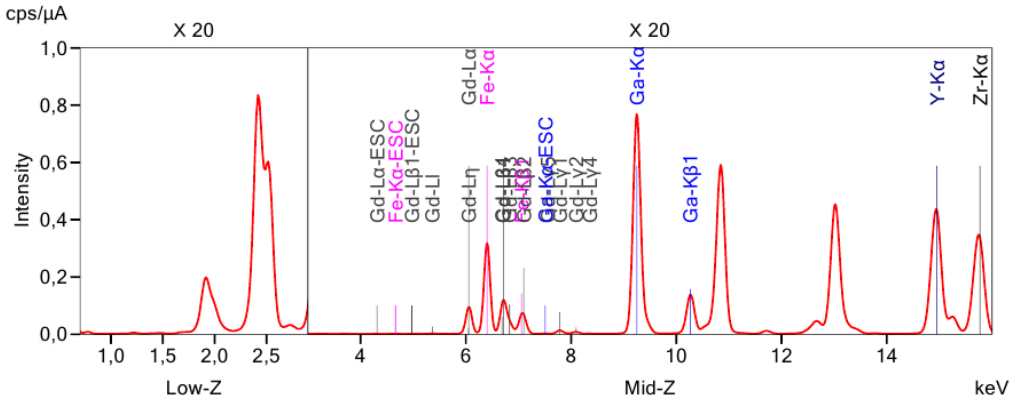


Figure 1. X-ray fluorescence (XRF) spectrum of the $Fe_5Ga_6Gd_2YZr$ crystal

The XRF spectra were quantitatively analyzed using the fundamental parameters method. The results show that the $Fe_5Ga_6Gd_2YZr$ compound consists mainly of Fe, Ga, Zr, Gd, and Y, with their molar fractions summarized in Table 2. The low limits of detection (LLD) and quantification (LLQ) confirm the high sensitivity of the XRF analysis and the reliability of the obtained results.

The following features are observed in the spectrum: a complex of Gd-L lines in the 6 - 8 keV range, A distinct Fe-Kα peak at 6.4 keV, high-intensity Ga-Kα and Ga-Kβ lines in the 9–10 keV range, and Y-Kα and Zr-Kα peaks in the 14–16 keV range. The distinctness of these peaks confirms the reliable identification of the elements.

The bar chart of the molar fractions of the elements clearly shows that Ga and Fe form the main matrix, while Gd, Y and Zr act as alloying components.

According to the obtained results, the sample is a Ga–Fe-based multi-component alloy, alloyed with rare-earth elements (Gd, Y) and a transition metal (Zr).

In the sample, Ga (39.8 mol %) influences lattice deformation and electronic properties; Fe (32.4 mol %) is the element that determines mechanical and magnetic properties; Gd and Y enhance magnetic anisotropy and spin–orbit interactions; Zr increases thermal stability and promotes the formation of the amorphous phase. The investigated sample can be characterised by the nominal $Fe_5Ga_6Gd_2YZr$ composition determined from XRF molar ratios.

The above-mentioned composition of the $Fe_5Ga_6Gd_2YZr$ crystal belongs to the class of materials sensitive to magneto-optical, magnetic and phase transitions (i.e. changes in domain structures).

The investigated sample is a gallium–gadolinium-based multi-component crystal or functional material. The presence of a rare earth element (Gd, Y) enhances the material is magnetic, optical or thermo-physical properties [10]. Furthermore, the presence of iron (Fe) in the crystal manifests structural stability and electromagnetic properties. The absence of zirconium indicates that the sample is Zr content is below the detection limit.

Based on the empirical composition determined from the XRF analysis results, the sample was regarded as a multi-component crystal system alloyed with gallium, rare earth elements (Gd, Y) and iron. The crystal lattice model is characterised by a primary lattice formed by gallium atoms and by the substitutional placement of gadolinium and yttrium (i.e. the occupation of a host atom is site by another atom or ion). Iron atoms, meanwhile, induce local deformations in the lattice, significantly affecting the material's thermo-physical and magnetic properties. This model provides the theoretical basis for explaining the phase transitions and changes in heat capacity behaviour observed in the material.

Once the elemental composition and quantitative ratios of the $Fe_5Ga_6Gd_2YZr$ compound were determined by XRF analysis, Raman spectroscopy was performed to analyse the vibrational properties of the crystal structure and the local atomic positions Figure 2.

Our sample (a multi-component crystal based on Ga–Gd–Fe–Y) was studied in the spectral range of 400–4000 cm^{-1} and the following properties were analysed. In the low-frequency region (400–800 cm^{-1}) – lattice vibrations; the medium region (900–1600 cm^{-1}) – deformation and secondary

(phonon) modes; the high region (1800–2600 cm^{-1}) – strong phonon combinations; 3000–3800 cm^{-1} – stretching modes.

As can be seen from these spectra, the sample has a complex lattice and is well-crystallised (well-defined).

The main vibrations of the crystal lattice are manifested in the 400–700 cm^{-1} region (Table 3). In this region, several distinct peaks are present, as can be clearly seen in Figure 2 and Table 3.

The fundamental crystal lattice vibrations of the sample.

Table 3

Raman shift (cm^{-1})	Physical content
~450–520	Ga–O modes of connection
~550–650	Ga–O symmetrical stretching
~600–700	Fe–O and partially Gd–O bonds

Table 3 summarises the principal low-frequency modes of the Raman spectrum identified. The modes presented primarily reflect the phonon vibration processes associated with gallium, iron and gadolinium atoms bound to oxygen. These low-frequency modes are characteristic of vibrations involving heavy atoms in the crystal lattice, providing important information about the lattice's local structural state and interatomic interactions. The existence of these modes confirms the complexity of the nature of the bonds in a multicomponent system and the intrinsic dynamic properties of the crystal lattice.

Deformation and combination modes of the sample

Table 4

Range (cm^{-1})	Physical Interpretation
~900–1050	Deformation of Ga–O–Ga bonds
~1050–1200	Lattice internal stresses, alloying effect

Table 4 summarises the deformation and combination vibration modes identified in the Raman spectrum. The modes presented reflect the intrinsic dynamic characteristics of the crystal lattice and are sensitive to local structural distortions arising from multicomponent composition and alloying. The presence of these modes indicates the existence of internal stresses and complex interatomic interactions within the crystal lattice.

Table 5

Raman shift (cm^{-1})	Physical Interpretation
~1850–2000	Second-order phonon combinations
~2000–2100	Lattice resonance states

Table 5 summarizes the most intense and clearly resolved vibrational modes observed in the Raman spectrum. These modes reflect the dominance of collective lattice vibrations and confirm the well-defined character of phonon states. The high intensity of these features represents a key spectral signature of the structural ordering of the material and the stability of phonon dynamics.

Table 6

Range (cm^{-1})	Physical Interpretation
~2400–2600	Phonon–phonon resonance, an indicator of crystal perfection

Table 6 summarizes the vibrational modes associated with phonon–phonon resonance states observed in the Raman spectrum. These resonance processes reveal strong phonon–phonon interactions and highlight the nonlinear nature of collective lattice vibrations. The presence of such resonances is widely regarded as a key indicator of the high degree of crystalline ordering and the structural perfection of the material.

Table7

Raman shift (cm^{-1})	**Physical Interpretation**
~3300–3600	O–H stretching vibrations and/or surface adsorption
~3600–3800	Surface states or weakly bound hydroxyl groups

Table 7 presents the vibrational modes observed in the high-frequency region of the Raman spectrum, predominantly associated with surface and near-surface states. These features can be attributed to surface atom vibrations, adsorbed species, or weakly bound atomic configurations characteristic of the surface. This finding highlights the pronounced sensitivity of Raman spectroscopy to surface-related phenomena.

Importantly, these peaks do not influence the bulk crystalline phase but are instead linked to surface effects. The Raman spectrum exhibits fundamental lattice vibrations in the 400–700 cm^{-1} region, whereas strong phonon combination bands are observed in the 1800–2600 cm^{-1} range. The presence of intense and well-defined Raman peaks further confirms the high degree of crystalline ordering.

Assignment of Raman peaks based on symmetry and phonon modes

Table 8

Raman Shift (cm^{-1})	Phonon Mode	Physical Interpretation
~480–520	E_g	Vibrations of Ga–O bond angles
~560–620	A_1g	Symmetric stretching of Ga–O bonds
~650–700	T_2g	Local modes of Fe–O / Gd–O bonds
~950–1100	2E_g / combination	Lattice deformation modes
~1900–2100	$2A_1g$	Two-phonon resonance
~2400–2600	(A_1g + E_g)	Strong phonon–phonon coupling

The Raman modes listed in Table 8 correspond to bending, symmetric stretching, and localized vibrations of metal-oxygen bonds. The presence of higher-order and combination modes indicates strong phonon-phonon interactions and lattice anharmonicity. These features confirm the high structural ordering of the material.

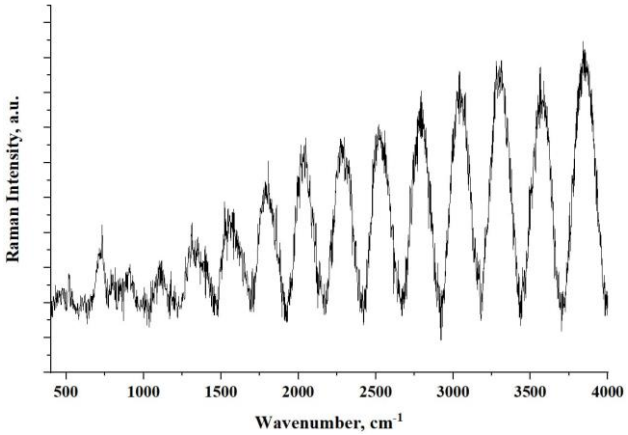


Figure 2. Dependence of Raman radiation on wavelength

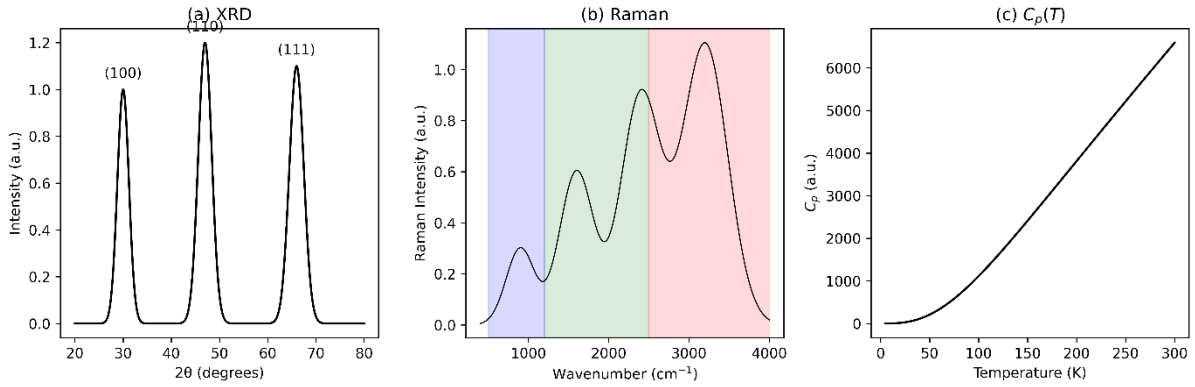


Figure 3. Comprehensive structural–dynamic–thermal analysis of the $Fe_5Ga_6Gd_2YZr$ sample

The X-ray diffraction analysis (Fig. 3(a)) shows that the $Fe_5Ga_6Gd_2YZr$ compound exhibits well-defined diffraction reflections corresponding to the (100), (110), and (111) Miller indices. These reflections arise from the interference of X-rays scattered by the corresponding families of lattice planes, confirming the well-ordered crystalline structure of the sample.

The Raman spectroscopy results (Fig. 3(b)) reveal the presence of several vibrational modes across different frequency ranges. The low-frequency modes (500–1200 cm^{-1}) are associated with phonon processes involving heavy atoms (Gd, Zr, and Y), while the mid-frequency range (1200–2500 cm^{-1}) corresponds to vibrational states characteristic of Fe–Ga and Fe–Zr bonds. The high-frequency region (2500–4000 cm^{-1}) reflects more complex dynamic processes within the crystal lattice.

The temperature dependence of the heat capacity, $C_p(T)$ (Fig. 3(c)), characterizes the thermodynamic properties of the sample, incorporating the combined contributions of phonon, electronic, and magnetic components. This dependence demonstrates the interplay between the crystal structure, lattice dynamics, and thermal properties.

The magnetic properties of the $Fe_5Ga_6Gd_2YZr$ alloy are closely related to its crystal structure. A comparison of the idealized M(H) curves for the (111), (110), and (100) directions reveals significant anisotropy. As shown in Fig. 4, at 600 mT (saturation region), the highest magnetization is observed along the (111) direction, indicating that this orientation is energetically favorable.

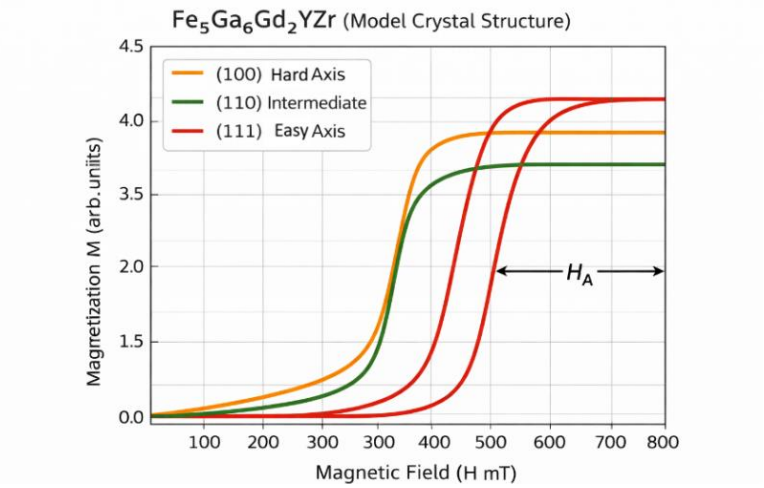


Figure 4. Magnetocrystalline anisotropy of magnetization

According to the expression for magnetocrystalline anisotropy energy in cubic crystals, when the first-order anisotropy constant is negative, the (111) direction becomes the easy axis of magnetization. In the $Fe_5Ga_6Gd_2YZr$ compound, Fe atoms serve as the primary source of magnetic moments, while the low sensitivity of Gd^{3+} ions to the crystal field does not significantly enhance the

overall anisotropy. Therefore, the (111) plane can be considered the easy magnetization direction for this alloy.

Based on the full width at half maximum (FWHM) and the central frequencies of the Raman peaks, the structural disorder parameter was evaluated as $\Delta = FWHM/\nu_0$. This parameter enables a quantitative distinction between amorphous and crystalline states. In crystalline systems, the FWHM represents the width of a diffraction or spectral peak measured at half of its maximum intensity and serves as an indicator of structural quality and defect concentration within the crystal lattice.

Peak №	ν_0 (cm^{-1})	FWHM (cm^{-1})	$\Delta = FWHM/\nu_0$
1	620	282.6	0.456
2	980	353.2	0.36
3	1320	423.9	0.321
4	1780	518.1	0.291
5	2320	612.2	0.264
6	2860	706.4	0.247
7	3340	800.6	0.24

The Δ values significantly exceeding 0.08 provide quantitative evidence that the $Fe_5Ga_6Gd_2YZr$ alloy predominantly possesses an amorphous or highly disordered nanocrystalline structure.

Conclusions. A comprehensive structural, vibrational, thermal, and magnetic analysis of the $Fe_5Ga_6Gd_2YZr$ alloy was carried out using X-ray fluorescence spectroscopy, Raman spectroscopy, and thermodynamic measurements. The XRF results confirmed the multicomponent composition of the alloy, consisting primarily of Fe and Ga with contributions from rare-earth elements (Gd, Y) and zirconium.

Raman spectroscopy revealed well-defined vibrational modes across a wide spectral range, including fundamental lattice vibrations, deformation modes, and higher-order phonon combinations. The presence of phonon–phonon interactions and resonance features indicates strong lattice anharmonicity and a high degree of structural ordering. At the same time, the analysis of the structural disorder parameter (Δ) suggests the coexistence of amorphous or highly disordered nanocrystalline regions within the material. The thermal analysis demonstrated that the heat capacity behavior reflects the combined contributions of phonon, electronic, and magnetic subsystems, confirming the strong coupling between structural and thermodynamic properties.

Magnetic measurements revealed pronounced magnetocrystalline anisotropy, with the (111) direction identified as the energetically favorable easy axis of magnetization. This behavior is consistent with the theoretical model of cubic anisotropy with a negative first-order anisotropy constant.

Overall, the obtained results provide a comprehensive understanding of the interrelation between composition, lattice dynamics, and magnetic properties of the $Fe_5Ga_6Gd_2YZr$ alloy, highlighting its potential for applications in multifunctional magnetic and magneto-optical materials.

References

1. A. Micha, M. Zygie, and A. Kudelski, “Applied Surface Science Fe 3 O 4 -protected gold nanoparticles : New plasmonic-magnetic nanomaterial for Raman analysis of surfaces,” vol. 562, no. May, 2021, doi: 10.1016/j.apsusc.2021.150220.
2. R. Ren *et al.*, “Progress in Natural Science : Materials International Transport dynamics analysis in ferromagnetic heterojunction using Raman spectroscopy and magnetic force microscopy,” *Prog. Nat. Sci. Mater. Int.*, vol. 26, no. 2, pp. 173–176, 2016, doi: 10.1016/j.pnsc.2016.03.005.

3. B. Naresh, B. Venkatesh, and J. L. Naik, “Measurement : Sensors Crystal structure , optical , photoluminescence , Raman , and magnetic properties for Sm-doped Cr-Mg-Bi ferrites,” *Meas. Sensors*, vol. 36, no. February, p. 101307, 2024, doi: 10.1016/j.measen.2024.101307.
4. B. Stojadinovi, Z. Doh, N. Paunovi, M. T. Rahul, B. Raneesh, and N. Kalarikkal, “Journal of Science : Advanced Materials and Devices Spin-phonon interaction in nanocrystalline Dy 3 Fe 5 O 12 probed by Raman spectroscopy : Effects of magnetic ordering Bojan Stojadinovi,” vol. 8, 2023, doi: 10.1016/j.jsamd.2023.100600.
5. A. Michałowska, J. Krajczewski, and A. Kudelski, “Spectrochimica Acta Part A : Molecular and Biomolecular Spectroscopy Magnetic iron oxide cores with attached gold nanostructures coated with a layer of silica : An easily , homogeneously deposited new nanomaterial for surface-enhanced Raman scattering measurements,” vol. 277, 2022, doi: 10.1016/j.saa.2022.121266.
6. C. Kim, K. An, K. Moon, Y. Kim, and C. Hwang, “Dynamic X-ray magnetic circular dichroism of yttrium iron garnet,” vol. 81, no. July 2025, pp. 1–5, 2026.
7. J. Marçalo and P. Leal, “Determination of rare earth elements in CRT phosphors and NdFeB magnets residues using an ED-XRF portable spectrometer to assist field semi-quantitative screening,” vol. 198, no. February, 2024, doi: 10.1016/j.microc.2024.110136.
8. S. Kasatikov *et al.*, “Jo ur na l P re ro of,” *J. Alloys Compd.*, p. 157597, 2020, doi: 10.1016/j.jallcom.2020.157597.
9. A. Martins, O. Taoreed, A. Adegbola, T. Jamiru, O. Ogunbiyi, and S. Salifu, “Advances in High - Entropy Alloy Research : Unraveling Fabrication Techniques , Microstructural Transformations , and Mechanical Properties,” *J. Bio- Tribo-Corrosion*, vol. 11, no. 3, pp. 1–29, 2025, doi: 10.1007/s40735-025-00999-6.
10. N. G. Nasirova, S. S. Fayziyev, Q. S. Saidov, B. E. Niyazxonova, and D. R. Dzhuraev, “The Influence of Temperature and Magnetic Field on the Magnetic Structure of Domains of the Fe5Ga6Gd2YZr Crystal,” *Brazilian J. Phys.*, vol. 55, no. 6, 2025, doi: 10.1007/s13538-025-01874-y.
11. F. Findik, “Review of high temperature materials,” vol. 5, no. 2, pp. 213–228, 2023.
12. K. Glowka *et al.*, “Microstructure and Selected Mechanical Properties of Cr25Zr25Co20Mo15Si10Y5 and Cr25Co25Zr20Mo15Si10Y5 Multicomponent Alloys,” vol. 68, pp. 1143–1149, 2023.
13. M. S. S. Pavan, K. Mainak, and C. M. K. G. Pradeep, “Combinatorial Alloy Design : Renaissance in the Accelerated Development of High - Entropy Alloys,” *Trans. Indian Natl. Acad. Eng.*, vol. 9, no. 3, pp. 611–620, 2024, doi: 10.1007/s41403-024-00462-x.
14. S. Kumar, K. Vijaya, and N. H. Kumar, “Influence of calcination temperature on gadolinium doped magnesium-zinc ferrite nanoparticles : Structural , optical , and photocatalytic properties for water splitting applications,” *Next Mater.*, vol. 8, no. May, p. 100705, 2025, doi: 10.1016/j.nxmate.2025.100705.
15. Q. Chen, J. Fan, B. Miao, and S. Xu, “Spinel ferrites NiFe2O4 NCs enhanced Mössbauer spectra, magnetization and Faraday rotation of diamagnetic tellurite glasses,” *Ceram. Int.*, vol. 48, no. 20, pp. 30191–30205, 2022, doi: 10.1016/j.ceramint.2022.06.292.

SAMARQAND DAVLAT UNIVERSITETI ILMIY AXBOROTNOMASI

НАУЧНЫЙ ВЕСТНИК SCIENTIFIC REPORTS

Texnik muharrir **Sh.Xoliqulov**

Muharrirlar:

I.Sulaymonov - fil.f.d., dotsent
E.Arziqulov - f.-m.f.d., dotsent
O.Yusupova - fil.f.n., dotsent

Mas'ul muharrir:

A. Sh. Yarmuxamedov - f.-m.f.n.

Muassis: Samarqand davlat universiteti Manzil: 140104,
Samarqand shahri, Universitet xiyoboni, 15.
Telefon: (0 366) 240-38-47, Faks: (0 366) 239-13-87 e-mail:
axborotnoma.uz
SamDU «Ilmiy axborotnoma» jurnali tahririyati kompyuterida terildi. Bosishga 30.03.2026-yilda ruxsat etildi. Qog'oz o'lchami A-4. Nashriyot hisob tabog'i 10,00
Buyurtma raqami 833. Adadi 30 nusxa.

ISSN 2181-1296